

High Resistivity Characteristics of the Sinter Dust Generated from the Steel Plant

Jae Keun Lee*[†], Ok Chun Hyun, Jung Eun Lee

School of Mechanical Engineering, Pusan National University

Sang Deok Park

*Mechanical & Electrical Engineering Team Steel Process & Automation Research Center,
Research Institute of Industrial Science and Technology*

The electrical resistivity of sinter dusts generated from the steel industry and coal fly ash from the coal power plant has been investigated using the high voltage conductivity cell based on JIS B 9915 as a function of temperature and water content. Dust characterization such as the chemical composition, size distribution, atomic concentration, and surface structure has been conducted. Major constituents of sinter dusts were Fe_2O_3 (40~74.5%), CaO (6.4~8.2%), SiO_2 (4.1~6.0%), and unburned carbon (7.0~14.7%), while the coal fly ash consisted of mainly SiO_2 (51.4%), Al_2O_3 (24.1%), and Fe_2O_3 (10.5%). Size distributions of the sinter dusts were bi-modal in shape and the mass median diameters (MMD) were in the range of 24.7~137 μm , whereas the coal fly ash also displayed bi-modal distribution and the MMD of the coal fly ash was 35.71 μm . Factors affecting resistivity of dusts were chemical composition, moisture content, particle size, gas temperature, and surface structure of dust. The resistivity of sinter dusts was so high as 10^{15} ohm \cdot cm at 150 $^\circ\text{C}$ that sinter dust would not precipitate well. The resistivity of the coal fly ash was measured 1012 ohm \cdot cm at about 150 $^\circ\text{C}$. Increased water contents of the ambient air lowered the dust resistivity because current conduction was more activated for absorption of water vapor on the surface layer of the dust.

Key Words : Resistivity, Electrostatic Precipitator, Sinter Dust, Coal Fly Ash, Chemical Composition

1. Introduction

Today there are thousands of electrostatic precipitators (ESPs) in operation for the control of emissions from steam generating power plants, cement kilns, sinter plants, and other industrial sources. Much emphasis has been placed on the fact that effective precipitation coincides with the occurrence of optimum amounts of electrical input in the corona process. While power input is

sometimes limited by structure or individual component defects, most limited power installations occur under conditions of excessive electrical resistivity of the collected material. In the design of electrostatic precipitators, the electrical resistivity of the dust is one of several important factors to be considered since the resistivity inversely influences the allowable electrical operating parameters.

Although ESPs have been and will continue to be the major particulate control device used in sinter plants, very little information exists in the literature about the performance of sinter plant electrostatic precipitators. This is understandable since most of the attention in the last few years has been given to coal fly ash electrostatic precipitators (Ku et al., 2000; Steelhammer, 1977).

[†] First Author

* Corresponding Author,

E-mail : jklee@hyowon.pusan.ac.kr

TEL : +82-51-510-2455; FAX : +82-51-512-5236

School of Mechanical Engineering, Pusan National University (Manuscript Received July 3, 2000; Revised February 12, 2001)

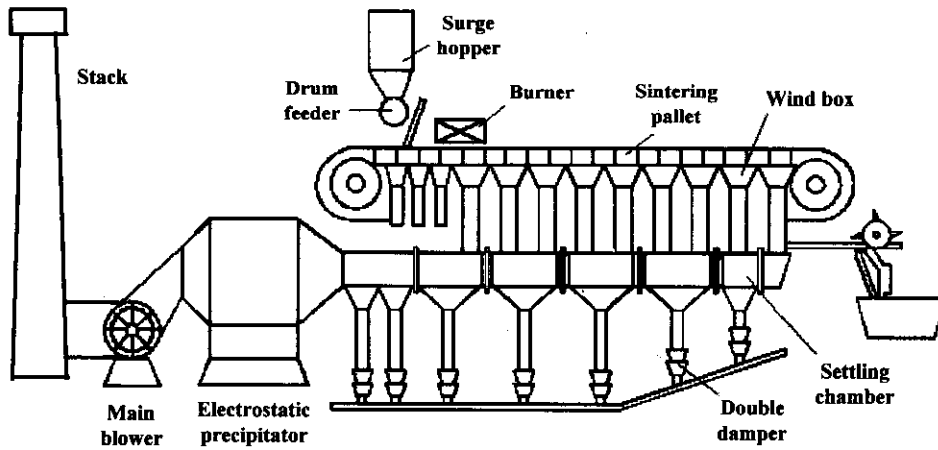


Fig. 1 Schematic diagram of the sinter process with the electrostatic precipitator in the steel industry

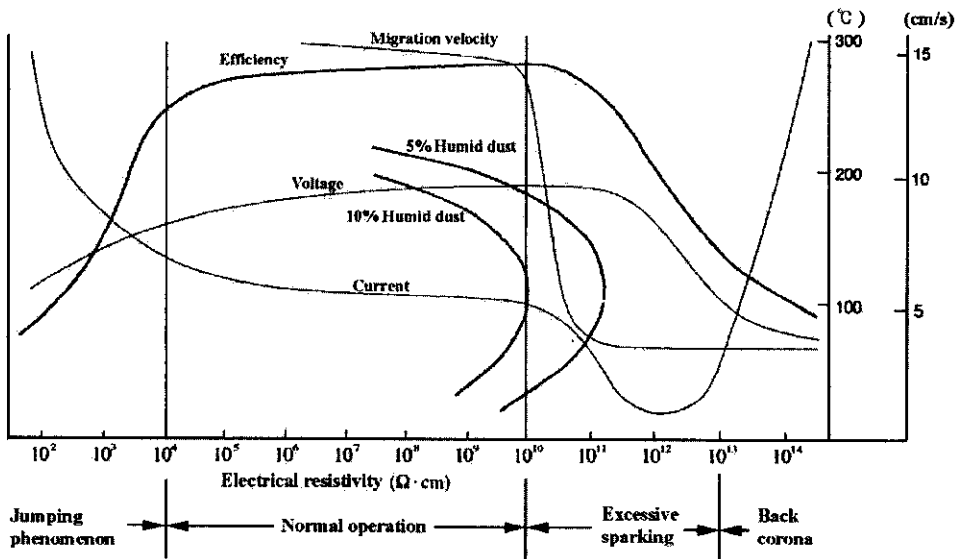


Fig. 2 Relationship of the dust resistivity and operation parameters in the electrostatic precipitator(Walker, 1968)

Therefore, most electrostatic precipitators were designed using the data based on the characteristics of coal fly ash such as electrical resistivity, chemical composition, size distribution, and so on. To design the ESP for some particulate emissions from an industrial process, it is necessary to get the information related to the emissions.

Iron ore in powdery form has to be sintered before it is fed to the blast furnace. Most sinter machines are Dwight Lloyd type where ore is fed

with powdery cokes and other materials to the upstream end of the moving pallet at which cokes are ignited. Combustion gas is exhausted downward through a number of wind boxes and lead to the sinter precipitator, as shown in Fig. 1 (Masuda, 1979). Briefly, sintering is a process for agglomerating iron-bearing fines to prevent their loss during reduction in the blast furnace. In this study, the sinter dusts are received from the sinter plant No. 1 at the Pohang steel industry in Korea.

The purpose of this study is to investigate the

characteristics of electrical resistivity in the sinter dusts generated from the steel industry and the coal fly ash from the coal power plant as a function of operating temperature and water content in the environment. Electrical resistivity has been determined by means of the high voltage conductivity cell based on the JIS B 9915. Dust characterization such as the chemical composition, size distribution, atomic concentration, and the surface structure have been conducted and analyzed.

2. Electrical Resistivity

Particle resistivity is a condition of the particle in the gas stream that can alter the actual collection efficiency of an ESP design. The most economical design and operation of an ESP are obtained when the electrical resistivity of the particulate is kept within certain limits. Resistivity is a term that describes the resistance of the collected dust layer to the flow of electrical current. By definition, the resistivity is the electrical resistance of a dust sample 1.0cm^2 in cross-sectional area, 1.0 cm thick, and recorded in unit $\text{ohm}\cdot\text{cm}$. It can be described as the resistance to charge transfer by the dust. Dust resistivity values can be classified roughly into three groups of low resistivity ($<10^4\text{ ohm}\cdot\text{cm}$), normal resistivity ($10^4\text{--}10^{10}\text{ ohm}\cdot\text{cm}$), and high resistivity regime ($>10^{10}\text{ ohm}\cdot\text{cm}$) (Beachler, 1981).

Figure 2 shows the general relationship between the electrical resistivity of dusts and the operation variables such as the ESP efficiency, migration velocity, corona voltage, and corona current (Walker, 1968). If resistivity is too low below $10^4\text{ ohm}\cdot\text{cm}$, particles reaching the collecting electrode rapidly lose their charge and become re-entrained in the gas. While resistivity is too high above $10^{10}\text{ ohm}\cdot\text{cm}$, particles are hard to charge, limiting power input. Particles are also slow to lose their charge when they reach the collecting electrode because of the low conductivity of the dust layer already deposited. This increases the voltage gradient across the deposited layer, reduces the charging and collecting fields, and decreases particle migration

velocity. If the particulate is very resistive or builds up enough, the voltage gradient across the dust layer causes a dielectric breakdown and a phenomenon called back corona in which ions of the charge opposite to those generated at the discharge electrode effectively neutralize the unipolar space charge and severely reduce collection efficiency.

3. Experimental Procedures

3.1 Dust analyzer

The sinter dusts used in this study were obtained at the 1st, the 2nd, the 3rd, and the 4th stage of the sinter precipitator in the steel industry and the coal fly ash from the coal power plant. The chemical composition, particle size distribution, atomic concentration, and the surface structure were investigated for dust samples. Chemical compositions such as SiO_2 , Al_2O_3 , and Fe_2O_3 were determined using an X-ray Fluorescence Spectrometer (Philips, PW 2400). A particle counter (Malvern, Mastersizer Micro plus) was used to determine the particle size distribution. Atomic concentration such as Fe, Li, Na, Ca, and Mg was determined using an Inductively Coupled Plasma Atomic Emission Spectrometer (Thermo Jarrell Ash, ICP-IRIS). The shape and surface structure of dust were investigated using a Scanning Electron Microscope (SEM) and an Energy Dispersive X-ray Spectrometer (HITACHI, S-4200).

3.2 Resistivity measurement

Figure 3 shows the high voltage conductivity cell used in this study for measuring the electrical resistivity of dusts. It is designed based on the Japanese Industrial Standard JIS B 9915 (JIS, 1989). The high voltage conductivity cell is composed of two parallel electrodes of a lower electrode loading a dust sample and an upper electrode placed on a dust layer. The lower electrode is composed of a main electrode and a guard electrode. The upper electrode is 35.7 mm in diameter and its total mass is 100 g .

Figure 4 shows the schematic diagram of a laboratory electrical resistivity measuring system.

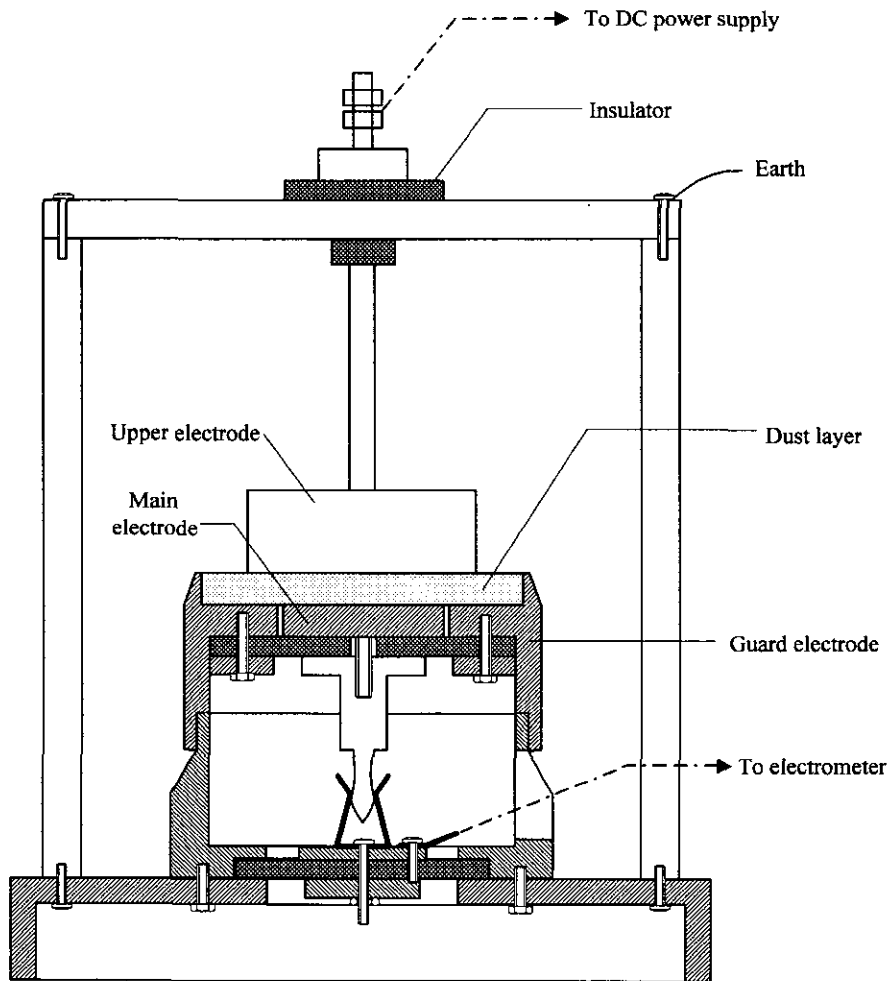


Fig. 3 Schematic diagram of the high voltage conductivity cell for measuring electrical resistivity of dusts (JIS B9915)

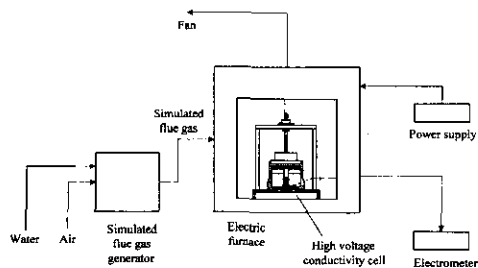


Fig. 4 Schematic diagram of the electrical resistivity test system with temperature and humidity control

It is composed of a high voltage conductivity cell, an electric furnace, a water vapor generator, a

high voltage power supply, and an electrometer. The temperature within the electric furnace can be held at any desired level between room temperature and 460°C by electric heaters, and the moisture content can be maintained at any selected value during the tests from the water content in the open air up to 40 vol.%. Dust resistivity is measured after initial temperature and water content are set and the temperature is held for not less than 30 minutes. And then temperature is increased to next measuring point. The currents are read 2 minutes later after the voltage of dc 2 kV is applied.

Resistivity of the dust is obtained from the

Table 1 Chemical characterization of the sinter dust and the coal fly ash

Chemical composition	Sinter dust				Fly ash
	Stage 1	Stage 2	Stage 3	Stage 4	
SiO ₂	6.0	5.0	4.5	4.1	51.4
Al ₂ O ₃	1.7	2.1	1.8	1.6	24.1
Fe ₂ O ₃	74.5	44.8	44.4	39.6	10.5
MnO	0.4	0.3	0.3	0.3	-
Li ₂ O	-	-	-	-	0.05
CaO	8.2	7.4	6.9	6.4	3.1
MgO	1.2	1.0	1.0	0.9	1.2
K ₂ O	0.1	9.2	10.0	12.4	2.9
Na ₂ O	0.10	1.15	1.15	1.28	0.66
P ₂ O ₅	0.1	0.2	0.2	0.2	0.3
TiO ₂	0.1	0.1	0.1	0.1	2.7
C	7.0	13.8	14.1	14.7	2.3

Table 2 Atomic concentration analysis of sinter dusts and coal fly ash relating to resistivity

Component	Atomic concentration(%)		
	Stage 1	Stage 4	Fly ash
Li	0.001	0.003	0.084
Na	0.02	0.76	0.53
Fe	54.20	29.38	1.97
Ca	5.82	4.46	2.07
Mg	0.69	0.51	1.12

experimental data of current density in a given electrical field strength as follows (JIS, 1989),

$$\rho_d = \frac{E}{J} \quad (1)$$

where ρ_d is the resistivity of the dust (ohm · cm). E is the electric field strength between two electrodes (V/cm) and J is the current density (A/cm²). Dust layer thickness is 0.5 cm and the cross-sectional area of the upper electrode is 5 cm². The applied voltage to the high voltage conductivity cell is 2 kV.

4. Results and Discussions

4.1 Dust characterization

Table 1 shows the results of the chemical characterization of the sinter dusts from the 4 stages of the ESP in the steel industry and fly ash

from the coal-fired power plant. The results of elementary chemical analysis are expressed in weight percent of oxides. Major constituents of sinter dusts were Fe₂O₃, CaO, SiO₂, and unburned carbon, while the coal fly ash consisted of mainly SiO₂, Al₂O₃, and Fe₂O₃. The 1st stage sinter dust was mostly made up for Fe₂O₃ (74.5%) and other main constituents of CaO (8.2%), SiO₂ (6.0%), and unburned carbon (7.0%). However, the rest stage sinter dusts consisted of Fe₂O₃ (39~45%), K₂O (9~12%), unburned carbon (14%), and the other constituents similar to the 1st stage sinter dust. On the other hand, the coal fly ash primarily consisted of SiO₂ (51.4%), Al₂O₃ (24.1%), and Fe₂O₃ (10.5%). There is a trend of decreasing resistivity with increasing Fe₂O₃ and increasing resistivity with SiO₂, Al₂O₃, CaO, and MgO.

Table 2 shows the atomic concentrations of sinter dusts and coal fly ash. The 1st stage sinter



(a) Sinter dust from the 1st stage of ESP



(b) Sinter dust from the 4th stage of ESP

Fig. 5 Scanning electron microscope photographs of sinter dusts

dust contained Fe (54.2%), Na (0.02%), Li (0.001%), Ca (5.82%), and Mg (0.69%), whereas Fe (29.38%), Na (0.76%), Li (0.003%), Ca (4.46%), and Mg (0.51%) were included in the 4th stage dust. However, the coal fly ash contained Fe (1.97%), Na (0.53%), Li (0.084%), Ca (2.07%), and Mg (1.12%). Chemical analyses of the sinter dusts showed that Fe concentration was much higher than that of the coal fly ash, but little Li was contained. Alkali metals on the ash surface acted as charge carriers and that the combined lithium and sodium correlated well with resistivity (Bickelhaupt, 1979).

Figure 5 shows the SEM photographs of the 1st stage and the 4th stage of sinter dust. The size of the 1st stage sinter dust was much larger than that of the 4th stage. The shapes of the 1st stage sinter dust particles were polygonal and non-

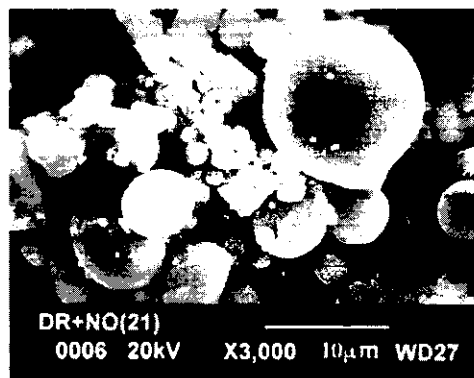


Fig. 6 Scanning electron microscope photograph of the fly ash

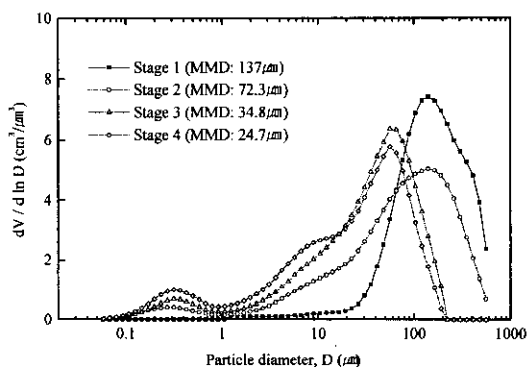


Fig. 7 Size distribution of the sinter dusts as a function of the ESP stage

combustive, otherwise the rest stages dust particles were shown in irregular forms and agglomerations occurred by the combustion of the ore, powdery cokes, and other materials. Figure 6 shows the SEM photograph of the coal fly ash generated from the coal fired power plant being in spherical shape commonly.

Figure 7 shows the size distributions of sinter dusts from each stage of ESP. The size distributions of the each stage sinter dust were bimodal in shape and the mass median diameters (MMD) of dusts in the 1st, 2nd, 3rd, and 4th stage were measured as 137, 72.3, 34.8, and 24.7 μm , respectively. Most large particles were collected in the 1st stage of the sinter ESP due to the gravitational settling, while smaller particles were captured in the rear stages. Figure 8 shows the size distribution of the fly ash generated by combustion of the mixture of NoVa coal and Drayton

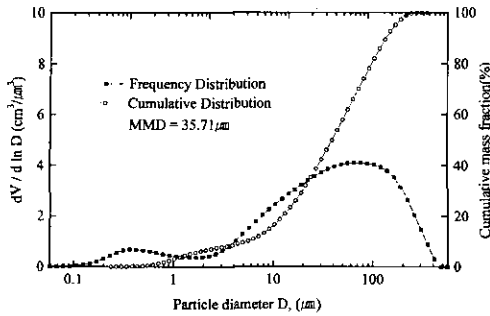


Fig. 8 Size distribution of fly ash generated from the mixture of Drayton coal and NoVa ash

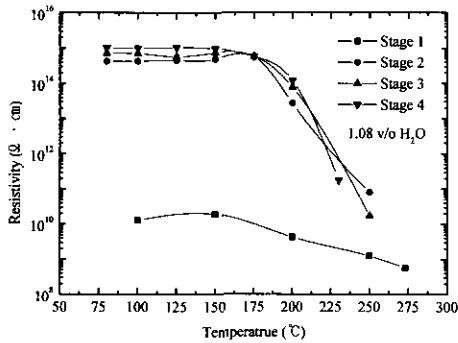


Fig. 9 Resistivity variation of the sinter dust at 1.08% water content as a function of ESP stage

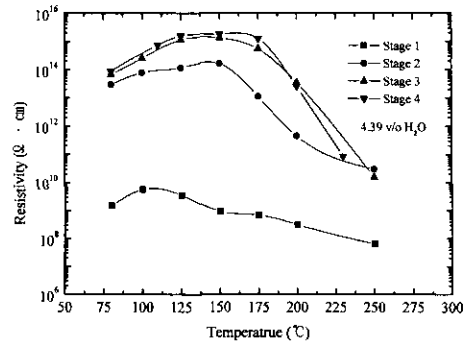


Fig. 10 Resistivity variation of the sinter dust at 4.39% water content as a function of ESP stage

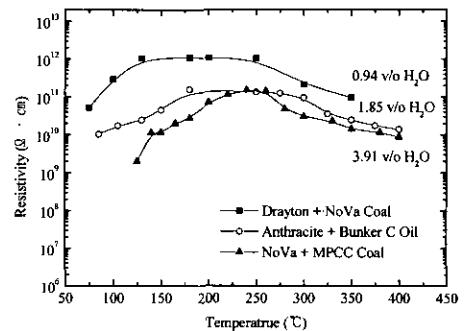


Fig. 11 Resistivity variation of the coal fly ash as a function of temperature and water contents

coal. This figure also displays bi-modal distribution and shows that the MMD of the coal fly ash was 35.71 μm .

4.2 Electrical resistivity of the sinter dust

Figure 9 shows resistivity curves of the 4 stages sinter dusts as a function of temperature at the water content of 1.08%. Figure 10 shows another set of resistivity curves at the water content of 4.39% for each stage in sinter ESP. At low temperature range of 80~150 $^{\circ}\text{C}$, the resistivity increased with temperature, while for high temperature above 150 $^{\circ}\text{C}$, it decreased steeply with increasing temperature. At low temperature range, current conduction occurs principally along the surface layer of the dust and resistivity is related to the absorption or adsorption of water vapor in the air. At high temperature range, conduction takes place primarily through the bulk of the dusts, therefore resistivity depends on the chemical composition of the material (Walker, 1968). The

resistivity of dust sampled at the rear stage of sinter ESP was higher than that of the front stage dust with the same water content and temperature of the air. When the water vapor content of the air was 1.08%, the resistivities of the 4 stage dusts in the vicinity of 150 $^{\circ}\text{C}$ were 9.25×10^8 , 1.61×10^{14} , 1.29×10^{15} , and 1.77×10^{15} ohm \cdot cm, respectively. On the assumption that back corona can be avoided for resistivities less than 10^{10} ohm \cdot cm, the 1st stage sinter dust should precipitate satisfactorily in the range of ESP operation temperatures regardless of water content. However, the rest stage sinter dusts probably would not precipitate well in the vicinity of operation temperatures due to the dust characteristics of high electrical resistivity.

Figure 11 shows the variation of the resistivity of the coal fly ash as a function of temperature for different mixture of coal ash and water content. The trend of resistivity curves agreed with that of

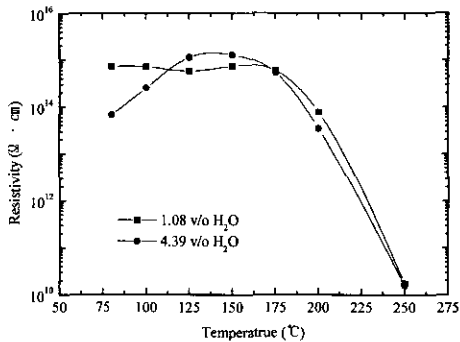


Fig. 12 Resistivity variation of the 3rd stage sinter dust as a function of temperature and water content

the sinter dusts. The highest resistivity of the mixture of Drayton and NoVa coal ash was about 10^{12} ohm · cm at 150 °C, the water content of 0.94%. Coal fly ash would precipitate quite well in the ESP since the resistivity of the coal fly ash is in the normal resistivity region.

Figure 12 shows the resistivity variations of the 3rd stage sinter dusts as a function of temperature at 1.08 and 4.39% water content. The dust resistivities for the 3rd stage at temperature 150 °C were 7.46×10^{14} ohm · cm at 1.08% water content and 1.29×10^{15} ohm · cm at 4.39% water content. Increased moisture content of ambient air lowered the dust resistivity at low temperature range because current conduction was more activated for absorption or adsorption of water vapor on the surface layer of the dust. Generally, for most of the common dusts collected by industrial precipitators, the operation becomes more efficient and trouble-free with increasing the moisture content of the gas by the use of water spray and steam injection.

The resistivities of the 1st stage sinter dust, the 4th stage sinter dust, and coal fly ash were as high as 10^{10} , 10^{15} , and 10^{12} ohm · cm, respectively, in the vicinity of ESP operation temperature of 150 °C. These differences in resistivity depend primarily on the chemical composition of the dusts. Dust resistivity decreased with increasing amounts of Na, Li, and Fe but increased with the amounts of Mg and Ca (Bickelhaupt, 1974). The resistivity was inversely proportional to the number of mobile charge carriers since lithium and

sodium ions were the principal charge carriers (Bickelhaupt, 1979). However, the quantitative contribution of the each element to the electrical resistivity has not been revealed. Besides the chemical composition of dusts, size distribution and surface structure of dusts have influence on the resistivity simultaneously.

5. Summary and Conclusions

The electrical resistivity of sinter dusts generated from the steel industry and coal fly ash from the coal power plant has been investigated as a function of temperature and water content. Electrical resistivity has been determined by means of the high voltage conductivity cell based on the JIS B 9915. Dust characterization with such as the chemical composition, size distribution, atomic concentration, and surface structure has been conducted.

Major constituents of sinter dusts were Fe_2O_3 , CaO, SiO_2 , and unburned carbon, while the coal fly ash consisted of mainly SiO_2 , Al_2O_3 , and Fe_2O_3 . Size distributions of the sinter dusts were bi-modal in shape and the MMD was in the large range of 24.7~137 μm , whereas the coal fly ash also displayed bi-modal distribution and the MMD of the coal fly ash was 35.71 μm . Chemical analyses of the sinter dusts showed that Fe concentration was much higher than that of the coal fly ash, but little Li was contained.

Factors affecting resistivity of dusts were chemical composition, moisture content, particle size, gas temperature, and surface structure of dust. Sinter dusts were classified as one of relatively low resistivity and the other of very high resistivity. The resistivity of sinter dust was so high as 10^{15} ohm · cm at 150 °C that sinter dust would not precipitate well due to the dust characteristics of high electrical resistivity. The resistivity of the 1st stage sinter dust was relatively low due to the high concentration of Fe. The resistivity of the coal fly ash was measured 10^{12} ohm · cm at about 150 °C.

The 1st stage dust at the water content of 1.08 and 4.39%, the resistivities at temperature 150 °C were 1.93×10^{10} and 9.25×10^8 ohm · cm.

Increased water content of the ambient air lowered the dust resistivity at low temperature range because current conduction was more activated for absorption or adsorption of water vapor on the surface layer of the dust.

Acknowledgements

This research was supported financially by the Research Institute of Industrial Science and Technology. The authors gratefully acknowledge the financial support.

References

- Beachler, S.D. and Jahnke, J.A., 1981, *APTI Course 4/3 Control of Particulate Emissions Student Manual*.
- Bickelhaupt, R.E., 1979, "A Technique for Predicting Fly Ash Resistivity," *Interagency Energy / Environment R&D Program Report*, U. S. EPA.
- Bickelhaupt, R.E., 1974, "Electrical Volume Conduction in Fly Ash," *Journal of the Air Pollution Control Association*, 27(2):114~120.
- Japanese Standards Association, 1989, "Measuring Methods for Dust Resistivity (with Parallel Electrodes) JIS B 9915," *Japanese Industrial Standard*.
- Ku, Jae Hyun, Lee, Jung Eun, and Lee, Jae Keun, 2000, "A Study of Fly Ash Resistivity Characteristics Generated from the Coal Fired Power Plant as a Function of Water Concentration and Temperature," *Transactions of the Korean Society of Mechanical Engineers*, Vol. 24, No. 4, pp. 526~532.
- Masuda, S., 1979, "Electrostatic Precipitation in Japanese Steel Industries," *Symposium on the Transfer and Utilization of Particulate Control Technology: Volume II*, pp. 309~318.
- Sproull, W.T. and Nakada, Woshinao, 1951, "Operation of Cottrell Precipitators, Effects of Moisture and Temperature," *Industrial and Engineering Chemistry*, Vol. 43, No. 6, pp. 1350~1358.
- Steelhammer, J.C., Nogash, D.R., and Polizzotti, D.M., 1977, "Laboratory Electrostatic Precipitator Studies Relating to the Steel Industry," *Proceedings: Particulate Collection Problems Using ESP's in the Metallurgical Industry*, pp. 54~71.
- Walker, A.B., 1968, "Operating Principles of Air Pollution Control Equipment," *Research Cottrell, Inc., Somerville, N.J.*